Received: 16 February 2024 | Accepted: 7 March 2024

DOI: 10.1002/ame2.12405

ORIGINAL ARTICLE

New insights into the interactions between the gut microbiota and the inflammatory response to ulcerative colitis in a mouse model of dextran sodium sulfate and possible mechanisms of action for treatment with PE&AFWE

Qianhui Fu | Xiaoqin Ma | Shuchun Li | Mengni Shi | Tianyuan Song | Jian Cui

Key Laboratory of Ethnomedicine of Ministry of Education, School of Pharmacy, Minzu University of China, Beijing, China

Correspondence
Jian Cui, Key Laboratory of Ethnomedicine of Ministry of Education, School of Pharmacy, Minzu University of China, Beijing 100081, China.
Email: cuijian9393@aliyun.com

Funding information
National Natural Science Foundation of China, Grant/Award Number: 81774449

Abstract

Background: Inflammatory bowel disease (IBD), comprising Crohn's disease (CD) and ulcerative colitis (UC), is a heterogeneous state of chronic intestinal inflammation. Intestinal innate immunity, including innate immune cells, defends against pathogens and excessive entry of gut microbiota, while preserving immune tolerance to resident intestinal microbiota, and may be characterized by its capacity to produce a rapid and nonspecific reaction. The association between microbiota dysbiosis and the pathogenesis of IBD is complex and dynamic. When the intestinal ecosystem is in dysbiosis, the reduced abundance and diversity of intestinal gut microbiota make the host more vulnerable to the attack of exogenous and endogenous pathogenic gut microbiota. The aim of our study was to comprehensively assess the relationship between microbial populations within UC, the signaling pathways of pathogenic gut microbe therein and the inflammatory response, as well as to understand the effects of using PE&AFWE (poppy extract [*Papaver nudicaule* L.] and *Artemisia frigida* Willd. extract) on UC modulation.

Methods: A UC mouse model was established by inducing SPF-grade C57BL/6 mice using dextrose sodium sulfate (DSS). Based on metagenomic sequencing to characterize the gut microbiome, the relationship between gut microbiota dysbiosis and gut microbiota was further studied using random forest and Bayesian network analysis methods, as well as histopathological analysis.

Results: (1) We found that the 5 gut microbiota with the highest relative abundance of inflammatory bowel disease UC model gut microbiota were consistent with the top 5 ranked natural bacteria. There were three types of abundance changes in the model groups: increases (Chlamydiae/Proteobacteria and Deferribacteres), decreases (Firmicutes), and no significant changes (Bacteroidetes). The UC model group was significantly different from the control group, with 1308 differentially expressed species with abundance changes greater than or equal to 2-fold. (2) The proportion of the

fecal flora in the UC group decreased by 37.5% in the Firmicutes and increased by 14.29% in the proportion of Proteobacteria compared to the control group before treatment. (3) The significantly enriched and increased signaling pathways screened were the 'arachidonic acid metabolic pathway' and the 'phagosomal pathway', which both showed a decreasing trend after drug administration. (4) Based on the causal relationship between different OTUs and the UC model/PE&AFWE administration, screening for directly relevant OTU networks, the UC group was found to directly affect OTU69, followed by a cascade of effects on OTU12, OTU121, OTU93, and OTU7, which may be the pathway of action that initiated the pathological changes in normal mice. (5) We identified a causal relationship between common differentially expressed OTUs and PE&AFWE and UC in the pre- and post-PE&AFWE-treated groups. Thereby, we learned that PE&AFWE can directly affect OTU90, after which it inhibits UC, inhibiting the activity of arachidonic acid metabolic pathway by affecting OTU118, which in turn inhibits the colonization of gut microbiota by OTU93 and OTU7. (6) Histopathological observation and scoring (HS) of the colon showed that there was a significant difference between the model group and the control group ($p < 0.001$), and that there was a significant recovery in both the sulfasalazine (SASP) and the PE&AFWE groups after the administration of the drug ($p < 0.0001$).

Conclusion: We demonstrated causal effects and inflammatory metabolic pathways in gut microbiota dysbiosis and IBD, with five opportunistic pathogens directly contributing to IBD. PE&AFWE reduced the abundance of proteobacteria in the gut microbiota, and histopathology showed significant improvement.

KEYWORDS
Arachidonic acid metabolism, Gut microbiota, Microbial dysbiosis, Proteobacteria

1 | INTRODUCTION

The intestinal microbiota is estimated to contain approximately 10^{14} commensal microorganisms, which are primarily bacteria localized in the distal ileum and colon.[1] The colon contains the highest microbial diversity and load, up to 10^{12} bacteria/g feces, and the microbial density also peaks in the colon.[2] The highly stable and shared component of microbiota between individuals is known as 'core microbiota'.[3] Although pathogens are rapidly recognized and destroyed by the immune response, the host tolerates the intestinal microbiota by mechanisms that are still unclear. On the one hand, the microbiota and the host form a symbiotic relationship. Human healthy individuals have high levels of interindividual variation in immune cell subset composition, while the microbiota can protect the host from opportunistic pathogenic infections.[4,5] Since they inhibit the adhesion to the gut mucus and colonization by pathogens, and bacteriocins and short-chain fatty acids,[6] the microbiota encodes hundreds of genes that do not exist in the human genome and regulates a variety of biological functions of the host, involving the absorption and digestion of nutrients, the maintenance of energy supply and the development of the immune system.[7,8] On the other hand, this tolerance can be disrupted, and evolve into an uncontrolled inflammatory response.[9] There are multiple causes of dysbiosis, such as imbalances in the composition of the gut microbiota, genetics of host–microbe interactions, etc.

Inflammatory bowel disease (IBD), characterized by chronic and relapsing inflammation of the gastrointestinal tract,[10] affects about 6.8 million people globally.[11] Individuals with IBD are at greater risk of developing colorectal cancer, called colitis-associated cancer, than normal individuals.[12] IBD not only affects the gastrointestinal (GI) tract but may also involve many other organs of the body,[13] for which the pathogenesis is either dependent on extended translocation of immune responses from the intestine, or is an independent perpetuated inflammatory event that shares a common environmental or genetic predisposition with IBD.[14] Several pathways by which the microbiota could contribute to IBD have been discussed in the past.[14] The idea that there is a molecular similarity between gut microbiota antigens and non-microbial epitopes on cells of affected organs has never been supported by clear evidence. Further evidence comes mainly from studies reporting on 'dysbiosis' and 'microbiota diversity', but these patients do not suffer from IBD. Disturbances or changes in the pathogenic and symbiotic microbiota are often referred to as 'dysbiosis'. This deregulation has multiple causes, but dysbiosis (an imbalance in the gut microbiota composition) and genes involved

in host–microorganism interactions have been associated with IBD,[15] supporting the importance of the microbiota and its interactions with the host in IBD pathogenesis.

The association of gut microbiota with IBD is strengthened by the fact that when germ-free mice are inoculated with IBD microbiota, they develop severe colitis.[16] Various murine models have been employed to evaluate factors that can alter the risk of IBD and to elucidate mechanisms of disease development and progression.[17] Our laboratory has used dextran sodium sulfate (DSS) to make an IBD model. Although most preclinical mouse models employed to evaluate factors do not fully recapitulate the complexity of human IBD, it remains unclear whether the currently accepted disorder of the gut microbiome is a cause or consequence of IBD. For this reason we have used DSS stimulation to simulate a model of disease onset and incorporate newly developed therapeutic approaches to provide new ideas for elucidating the mechanisms of IBD onset and for therapeutic strategies. A complete cure for IBD is unknown. The current treatment regimen using sulfasalazine (SASP) as a positive drug, is adopted to reduce inflammation, promote clinical remission, and prevent disease relapse.[18] However, the first-line treatment drugs currently used are usually accompanied by serious adverse reactions (such as allergies, intolerance, liver and kidney damage),[19,20] and the recurrence rate after treatment is high, with a recurrence rate of about 30%–40% within one year.[21,22] Fecal microbiota transplantation (FMT) interventions have also gained much attention as a novel therapeutic option for IBD.[23] The drug PE&AFWE contains extracts from *Papaver nudicaule* (*P. nudicaule* L.) and *Artemisia frigida* (*A. frigida* Willd.). The main active ingredient of *P. nudicaule* extract is alkaloids, which can antagonize the binding of leukotrienes and their receptors to prevent inflammatory reactions. The main chemical components of *A. frigida* are flavonoids, which also have good anti-inflammatory effects and can inhibit tumor necrosis factor α (TNF-α), interleukin-1β (IL-1-β), and prostaglandin E2 (PGE2). In the early stages of this study, pharmacological studies on the two extracts confirmed that they have good therapeutic effects on ulcerative colitis (UC), as part of which the lipid soluble alkaloids can play an antidiarrheal role.

To overcome the drawbacks in DSS modeling (the development of induced colitis does not require the involvement of T- and B-cells, whereas the pathological changes in DSS modeling more closely resemble those of human disease), firstly, we developed a stable immune-involved model of IBD by extending the stimulation of the modeling through three cycles, by selecting C57BL/6 mice. Mice that develop inflammatory colitis have differences in the composition of the gut microbiome during the early inflammatory phase compared to mice from other types of UC mouse model. Although these data suggest that the gut microbiome plays a role in IBD, we have not been able to determine a causal relationship between the microbiome and IBD. It is hypothesized that certain strains of gut microbes play a key pathogenic role in the development of IBD, and in order to gain a comprehensive understanding of the properties of gut microbes, a mouse model was designed, fabricated and studied.

2 | METHODS

2.1 | Chemicals

Dextran odium sulfate (36000–50000 MW; MP Biomedicals, USA), 70% ethanol, Genomic DNA Extraction Kit (DP304; Tiangen Biochemical Technology Co., Ltd, China).

2.2 | Laboratory animals

A total of 40 C57BL/6 mice, SPF grade, weighing 22 ± 2 g, 7 weeks old (Huafukang Biotechnology Co., Ltd; license number: SCXK [Beijing] 2019-0008). Three to five mice per cage were housed in the SPF Laboratory Animal Facility (SYKX [Tianjin] 2021-0003; Prebiotic Gene Technology Co., Ltd). All mice were kept at 24 ± 1°C, 54 ± 2% humidity, and a 14:10 h light:dark cycle. Food and water were provided ad libitum. All experimental measures were carried out in accordance with the approved guidelines (*Guide for the Care and Use of Laboratory Animals*) formulated by the China Animal Protection Committee (Tables 1 and 2).

2.3 | Composition and preparation of PE&AFWE

The drug PE&AFWE contains extracts from *P. nudicaule* L. and *A. frigida* Willd. Crude drugs were purchased from the Neimenggu autonomous region traditional Chinese medicine procurement and supply company. The *P. nudicaule* L. and *A. frigida* Willd. were mixed

TABLE 1 Scoring of disease activity index.

Observation index	0	1	2
Weight change	Increase or decrease <5%	Increase or decrease 5% ≤ 10%	Increase or decrease >10%
Hair condition	Neat and shiny	Messy and shiny	Messy and matte
Activity	Normal	Less activity	Inactive
Fecal shape	Well-formed	Loose stool	Liquid stool
Stool with mucus	None	Small amount	Mass
Stool with pus	None	Small amount	Mass
Stool with blood	None	Visible small amount to the naked eye	Clearly visible to the naked eye

TABLE 2 Histopathological score.

Category	0	1	2
Infiltration of acute inflammatory cells	None	Mild increase	Severe increase
Infiltration of chronic inflammatory cells	None	Mild increase	Severe increase
Submucosal edema	None	Mild increase	Severe increase
Epithelial cell necrosis	None	Limit	Diffuse
Ulcer formation	None	Have	

with a weight ratio of 15 g:24 g and then 22 volumes of 70% ethanol were added to reflux the mixture for 5 h. The combined extract was reduced to give a crude drug concentration 0.59 g/mL and stored in the dark at 4°C.

2.4 | Replication of UC model and administration

The establishment of the UC model was divided into three cycles. In the first cycle, mice received a 2.0% w/v DSS (MW 36000–50000; MP Biomedicals, USA) ad libitum solution for 7 days. The mice then received normal sterile drinking water ad libitum for the next 7 days. In the second cycle, mice were given a 1.5% w/v DSS drinking solution ad libitum for 7 days, after which they were given normal sterile drinking water ad libitum for another 7 days. In the third cycle, the mice were given 2.0% w/v DSS solution ad libitum for 2 days, then 1.5% w/v DSS ad libitum for another 5 days, and then sterile drinking water for another 2 days. The control group was given sterile drinking water.

The mice were euthanized, after the UC model was established, After cervical dislocation, the colon was excised and prepared for histopathological examination. After approval, the experimental protocol was carried out according to the guidelines formulated by the ethics committee of China University for Nationalities (protocol number: ECMUC2021006AO).

There were four groups, $N=10$ for each group: control group, UC model, sulfasalazine group (0.61 g/kg) and PE&AFWE group (5.07 g/kg). During the process of model establishment, each group was given its corresponding drugs. The administration route was intragastric. The model group was also gavaged with sterile drinking water. Consistency of external conditions between the groups of mice was ensured.

2.5 | Isolation of colonic lumen contents

The mice were euthanized and the colon segments were collected for longitudinal dissection in clean bench. The contents and fecal samples were collected and placed in 2 mL sterile cryotubes. Each sample was prepared with approximately 1 μg of DNA, frozen in liquid nitrogen and stored at −80°C. The above steps are carried out in clean bench.

2.6 | DNA extraction

PowerOil was used according to the manufacturer's instructions® Total genomic DNA was extracted from fecal samples with a DNA isolation Kit (MO BIO Laboratories). The Qubit dsDNA HS assay kit was used to detect the quality and quantity of extracted DNA on a qubit 3.0 fluorometer (Life Technologies, Carlsbad, CA, USA), and electrophoresis was performed on 1% agarose gel.

2.7 | Metagenomic analysis

Fecal DNA was isolated as described above. Whole genome shotgun libraries were prepared using the VAHTS Universal Plus DNA library preparation kit for Illumina (Vazyme Biotech). The paired ends of the library were sequenced using the 150 BP paired end sequencing mode on the Illumina Novaseq 6000 platform (Biomarker Technologies Co., Ltd, Beijing, China). Illumina raw reads were fine tuned for quality and adapter removal using Trimmomatic v0.33. After trimming the adapters and filtering the low-quality reads, the clean sequence data were used for further bioinformatics analysis. Sequence data associated with this project have been deposited in the NCBI short read archive database. The corresponding species information obtained after sequencing was analyzed for species composition and the abundance distribution of species was obtained by drawing a network diagram. Then, a Venn diagram was used to show the unique microbial species in each group and the microbial species shared by various groups. Using multiple sequence alignment and phylogenetic tree construction of microbial species, the differences in microbiota among different samples were found, and the principal coordinate analysis (PCoA) and nonmetric multidimensional scale (NMDS) dimensionality reduction map was used for analysis. We applied the metagenomic data analysis method (DESeq2) and rank sum test, followed by the linear discriminant analysis effect size (LEfSe), to statistically analyze samples. The screened differentially expressed microorganisms were assigned operational taxon unit (OTU) to machine learning, and the putative representative classification of OTUs were annotated. Based on previous identification of microbial differences, random forest and Bayesian Causal Network Analysis machine learning methods were used to infer the interaction and causality between microorganisms.

2.8 | Construction of unigenes and taxonomic prediction

Metagenemark was used to predict the open reading frame (ORF) of each assembled contig (Zhu W, Lomsadze A, Borodovsky M. Ab initio gene identification in metagenomic sequences. *Nucleic Acid Res*. 2010;38(12):132) (http://exon.gatech.edu/meta_gmhmmp.cgi,

version 3.26, default parameters), redundant genes (95% identity, 90% overlap) were removed by mmseqs2 software (https://github.com/soedinglab/mmseqs2, version 12-113e3), generating nonredundant gene catalogs (Steinegger M, Soding J. mmseqs2 enables sensitive protein sequence searches to be used for the analysis of massive datasets. *Nat Biotechnol*. 35:1026–1028). The reads were aligned using diamond software for classification function assignment and classification.

2.9 | Gene function annotation

KEGG annotation was performed against the Kyoto Encyclopedia of genes and genomes database using diamond (version 0.9.29) (http://www.genome.jp/keeg/). The *E*-value cutoff is 1e-5. If there are multiple alignment results (HIT), the best alignment result is selected as the annotation of the sequence. R studio and python were used to visualize the results of the analysis.

2.10 | Data analysis and statistics

The data are expressed as the means ± SEM, using GraphPad Prism (version 9.0) and SPSS (version 23.0). Parametric and nonparametric tests (including Wilcoxon rank sum test and *t* test) were used to analyze the abundance differences between microorganisms as well as gene functions. Unless otherwise stated, an adjusted p value < 0.05 should be considered statistically significant.

3 | RESULTS

3.1 | DSS stimulation was used to establish a mouse model of IBD, which was used as a basis for a comprehensive understanding of the relationships between gut microbiota in disease models and decreased diversity of the microbiome, microbial dysbiosis

Firstly, we established a UC model of inflammatory bowel disease (IBD) using dextran sodium sulfate (DSS) stimulation in C57BL/6 mice and the results are shown in Figure 1A,B. In the model, the top 5 gut microbiota in relative abundance in the mouse gut (natural gut microbiota Chlamydiae, Bacteroidetes, Firmicutes, Proteobacteria and Deferribacteres), when observed at the phylum level versus the genus level, revealed that the Bacteroidetes had reduced interactions with other phyla, and the Ascomycota no longer correlated with the other phyla. In the control group, the phyla Actinobacteria and Ascomycota and Proteobacteria were closely associated with Bacteroidetes and Firmicutes.

In the model we compared the different groups according to the different levels of gut microbiota and found that the top 5 gut microbiota in relative abundance in the mouse gut can be observed at the phylum level versus the genus level (Figure 1A,B), which is consistent with the rankings of the natural bacterial community as Chlamydiae, Bacteroidetes, Firmicutes, Proteobacteria and Deferribacteres. Figure 1C–E shows that Chlamydiae abundance increased, Bacteroidetes abundance did not change much, Firmicutes abundance decreased significantly, and at the family level, Chlamydiaceae abundance increased, and Muribaculaceae abundance decreased, Lachnospiraceae and Clostridiaceae abundance significantly decreased and Bacteroidaceae significantly increased. At the genus level, except for Chlamydia and Bacteroides which increased in abundance compared to the normal control, Clostridium and Prevotella decreased in abundance and Mucispirllum increased in abundance.

Using principal coordinate analysis (PCoA) and nonmetric multidimensional scaling (NMDS) analyses for β diversity analysis, the results showed that the number of gut microbiota shared by the UC model group and the normal control group was lower, and the number of differing species was higher (p value < 0.05). There was a significant difference in community structure (p value < 0.05), which proved the reliability of group differences in this experiment (Figure 1F–H).

We used Venn diagrams to show the microbial communities at the species level, and the results showed that there were significant differences between the UC model group and the control group, with 1308 differentially expressed species with abundance changes greater than or equal to 2-fold.

Among all species, in the UC model group (Figure 1I,J), 169 species were significantly up-regulated, 1144 species were significantly down-regulated, and the overall microbial abundance was reduced in the UC model group.

3.2 | Use of PE&AFWE treatment in a mice model of inflammatory bowel disease to observe changes in the gut microbiota

In our established mouse model, microscopic HE staining of colon sections showed severe structural destruction of the colon, destruction of crypts, loss of glands, visible ulcer formation in the intestinal wall, and infiltration of peripheral tissues with inflammatory cells. In the control group, the colonic mucosa and the structure of each layer were intact and normal (Figure 2A,B).

Before and after treatment with PE&AFWE, the three groups – the UC group, control group, and PE&AFWE group – were compared; there were differences at both the phylum level and the species level. The proportion of the Firmicutes in the UC group decreased by 37.5% and the proportion of Proteobacteria increased by 14.29% in the fecal microbiota of the UC group compared to the control group before treatment. *Lachnospiraceae* bacterium a4 was reduced in abundance and *Chlamydia abortus* was the most abundant. After the treatment, the abundance of Proteobacteria in the UC group decreased by 14.29%, the abundance of the Firmicutes increased by 25%, and the proportion of the Bacteroidetes decreased

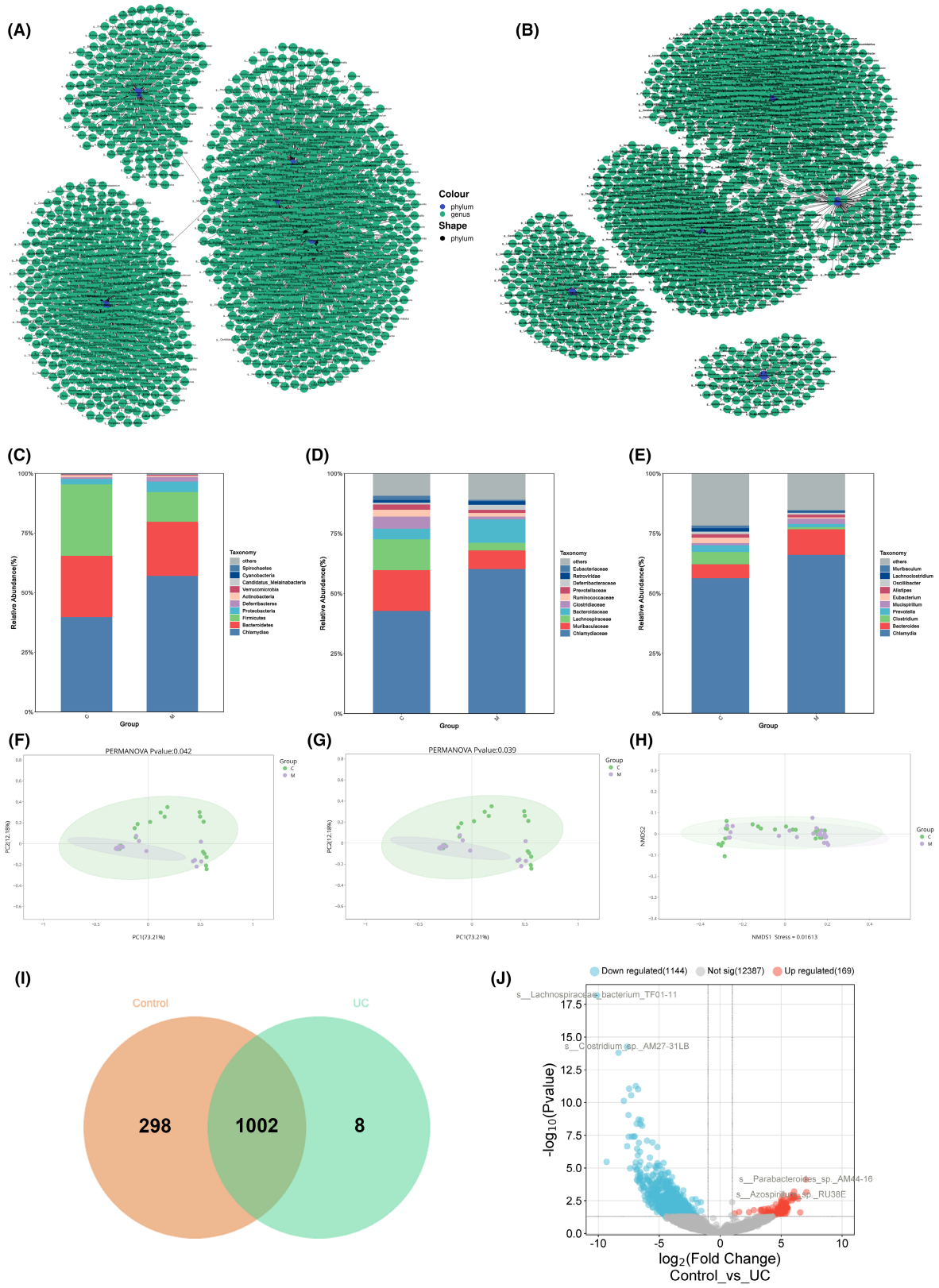

FIGURE 1 The level and genus of colonic microbiota of normal mice changed after DSS stimulation, and the colonic microbiota of mice in UC model group changed differently. (A) Network diagram between microbiota and genus of mice in the normal control group. (B) Network diagram between microbial phyla and genera in DSS stimulated model group mice. (C–E) Histograms at phylum level (C), family level (D), and genus level (E) in the two groups of mice. (F–H) Principal coordinate analysis PCoA plot, anosim analysis (F), PerMANOVA analysis (G), nonmetric multidimensional scale NMDS analysis (H) were used for the normal control and UC model groups. (I) Venn diagram of microorganisms with significant differences between the two groups. (J) Volcano diagram of species difference change in UC model group compared with control group. C, control; M, UC model. Blue nodes represent the phylum level and green nodes represent the genus level.

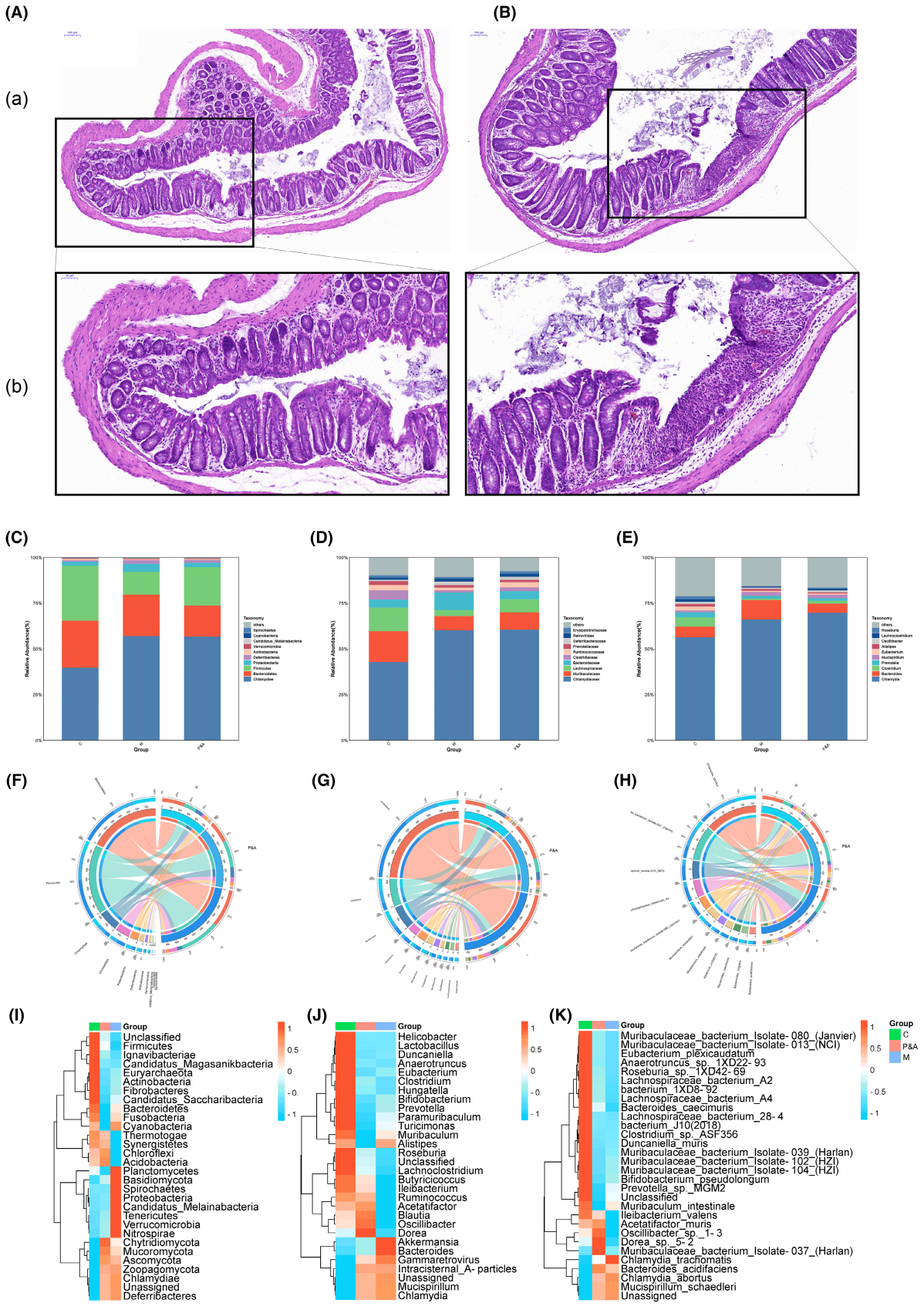

FIGURE 2 PE&AFWE regulates the composition of intestinal microbes in mice after administration. (A, B) Pathological staining diagram of colon in control group (A) and the DSS + UC model group (B). (a) The upper image is 10× (scale bar:100 μm); (b) the lower image is 20× (scale bar: 50 μm). (C–E) Bar graphs for three groups of mouse at the phylum level (C), family level (D), and genus level (E). (F–H) The Circos ring diagram of phylum level (F), genus level (G) and species level (H) differences. (I–K) The heatmaps of top 30 species at phylum level (I), genus level (J) and species level (K) among the three groups showed the related abundances. C, control; M, UC model; P&A, PE&AFWE group.

by 3.45% (Figure 2F–H), whereas the abundance of *Lachnospiraceae* bacterium a4 and *Muribaculaceae* bacterium Isolate-037 (Harlan) increased in the PE&AFWE group. We verified the reliability of the results by visualizing them to show the consistency of the Heatmap map with the CIROS map.

3.3 | Changes in gut microbial diversity in a mouse model of inflammatory bowel disease were associated with its differential microbiota, and further comprehensive analyses revealed dysbiosis-associated inflammatory pathways

We went on to investigate the similarity in the flora between the different groups using PCoA and NMDS methods. As shown in Figure 3, the PE&AFWE administration group had a lower number of shared species, a higher number of differential species, a significant difference in community structure, and the reliability of grouping differences ($p = 0.012$, Stress = 0.0172) compared to the UC model group. KEGG analysis screened 858 gut microbiota associated with the inflammatory pathway.

In the PE&AFWE administration group (1) 339 microbial species were significantly changed, and the Firmicutes/Bacteroidetes ratio in the gut was significantly higher after administration (Figure 3E), whereas the Firmicutes/Bacteroidetes ratio was reduced in the model group; (2) 138 microbial community species levels were significantly changed in the intervention, and the change in abundance was greater than or equal to 2-fold that of the model group; (3) 51 species were significantly up-regulated after administration of the drug, and 294 species were significantly downregulated (Figure 3G).

Prior difference analysis of the UC model group compared to the control group showed 1038 differentially expressed microbes, and KEGG analysis was also performed showing that 858 differentially expressed microbial species were significantly correlated with 141 signaling pathways ($r > 0.6$, $p < 0.05$). 141 were correlated with inflammatory response pathways. In conclusion, the classification according to the operational taxonomic unit (OTUs) (Figure 3H) showed that the significantly enriched and increased signaling pathways screened were the 'Arachidonic acid metabolism' and 'Phagosome', which both showed a decreasing trend after drug administration (Figure 3I).

3.4 | Causal relationships between key differentially expressed microbial OTUs

In order to further investigate the comparison of key microbial species associated with UC before and after treatment by PE&AFWE. Using random forest and Bayesian network models, overlap was analyzed using supervised classification methods and the importance of species was ranked according to the random forest MeanDecreaseAccuracy score as the degree of contribution of OTUs (Table S2). The results showed that OTU54 > OTU12 > OTU93 > OTU69 > OTU7 > OTU121, with OTU90 having the greatest impact (Figure 4A). OTU90, OTU27 and OTU118 were negatively correlated with the phagosome pathway ($r = -0.6$, $r = -0.65$, $r = -0.62$, $p < 0.001$), and the rest were positively correlated ($r > 0.6$, $p < 0.001$, Figure 4B), and causal relationships between 20 key differentially expressed OTUs and UC and PE&AFWE were identified (Figure 4C,D).

Based on the causal relationship between different OTUs and the UC model/PE&AFWE administration, the OTU network was screened for direct correlation. The UC group directly affected OTU69, followed by a cascade of effects on OTU12, OTU121, OTU93, and OTU7, which may be the pathway of action that initiated the pathological changes in normal mice (Figure 4E). OTU90 was directly affected in the PE&AFWE group, followed by a cascade of effects on OTU27, OTU23 and OTU19, which may be the mechanism for the therapeutic effect of PE&AFWE in the UC model (Figure 4F).

3.5 | A Bayesian network was used to analyze the causal relationship between microbiota in two groups of models of the same disease (the UC model and the PE&AFWE group)

Signaling pathways and correlation analyses between major gut microbiota before and after PE&AFWE treatment were constructed using a Bayesian network analysis model. The results showed that we identified a causal relationship between common differentially expressed OTUs in UC group in the pre- and post-PE&AFWE-treated group (Figure 5B). Thereby, we learned that PE&AFWE can directly affect OTU90 after which it inhibits UC, which inhibits the activity of arachidonic acid metabolic pathway by affecting OTU118, which in turn inhibits the colonization of gut microbiota in the gut by OTU93 and OTU7.

Meanwhile, we learnt that the OTUs associated with UC and PE&AFWE are divided into two negatively correlated categories, namely OTU69/OTU12/ OTU121/OTU93/ OTU7 and OTU23/ OTU19/OTU25/OTU90/OTU27/OTU118, as shown in Figure 5A. The increased abundance of OTU90 was significantly different before and after PE&AFWE administration (Figure 5F) ($p < 0.05$). The change in abundance of these 11 key OTUs in the model group was reversible after administration.

In order to clarify the biomarkers of the different groups at three different levels, we applied LEfSe analysis to classify the 11 OTUs in the three groups: OTU90 and OTU23 in the PE&AFWE administration group, OTU69, OTU93, OTU12, OTU121, and OTU7 in the model group, and OTU118, OTU25, OTU19, and OTU27 in the PE&AFWE, control group. The OTUs associated with the PE&AFWE administration group were not related to arachidonic acid and were closely related to the phagosome pathway (Figure 5D,E). The five OTUs directly associated with the UC model group were significantly enriched in the arachidonic acid metabolic pathway (Figure 5C).

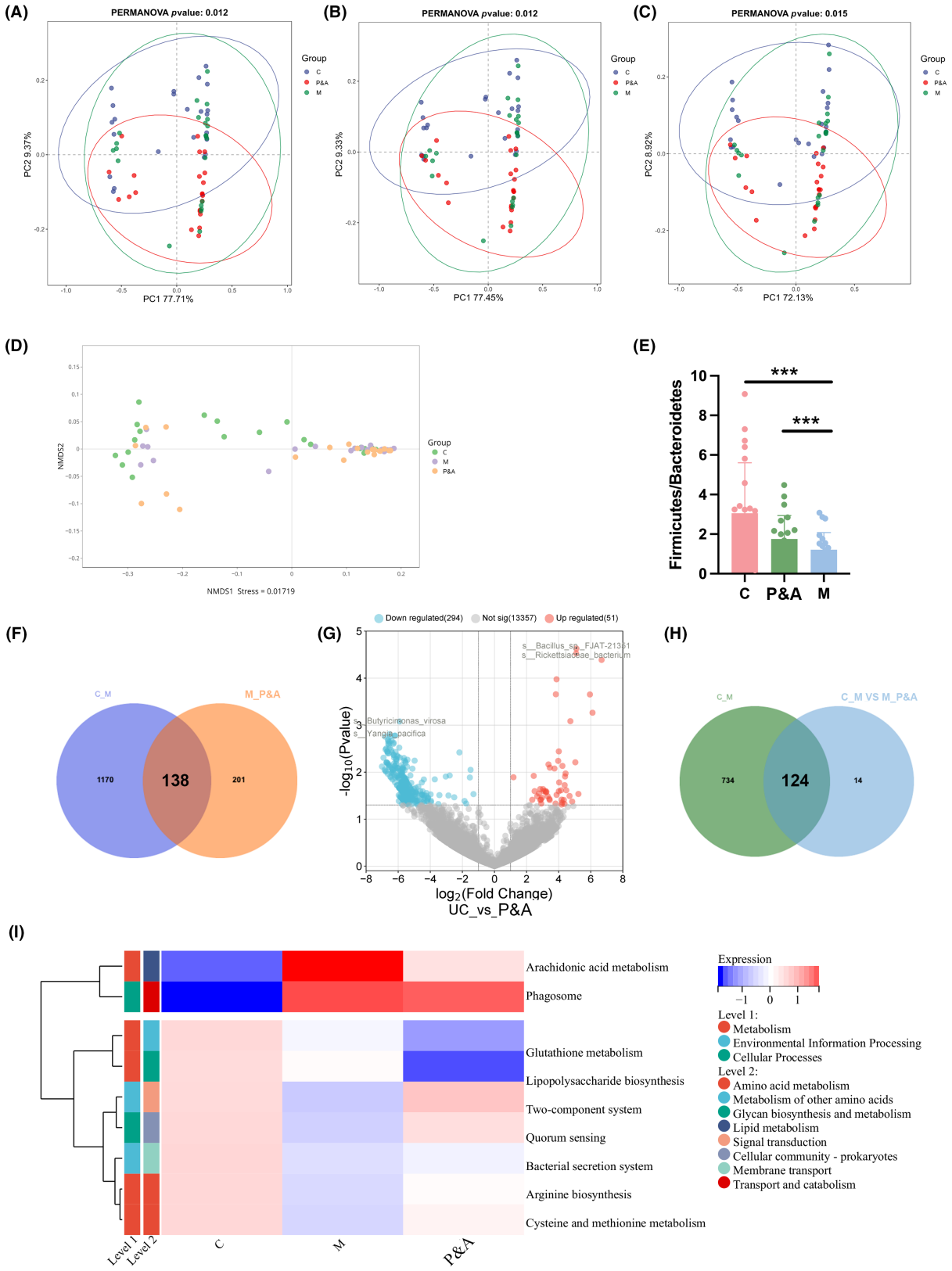

FIGURE 3 Changes in intestinal microbial diversity and differential expression of microorganisms after PE&AFWE administration. (A–C) Phylum level (A), genus level (B) and species level (C) PCoA diagram based on Bray Curtis principal coordinate analysis. (D) Nonmetric multidimensional scale NMDS analysis was used for the three groups. (E) Bar chart of the ratio of Firmicutes/Bacteroidetes in the three groups of mice. (F) The Venn diagram of microbiota was changed by the difference in microbiota and model group after administration. (G) Volcano diagram of species difference change after administration compared with UC model group. (H) The Venn diagram of microbiota was changed by the difference in microbiota and model group after administration related to the KEGG pathway. (I) The three groups compared. Compared with the model group, $^{*}p < 0.05$, $^{**}p < 0.01$, $^{***}p < 0.001$. C, control; M, UC model; P&A, PE&AFWE group.

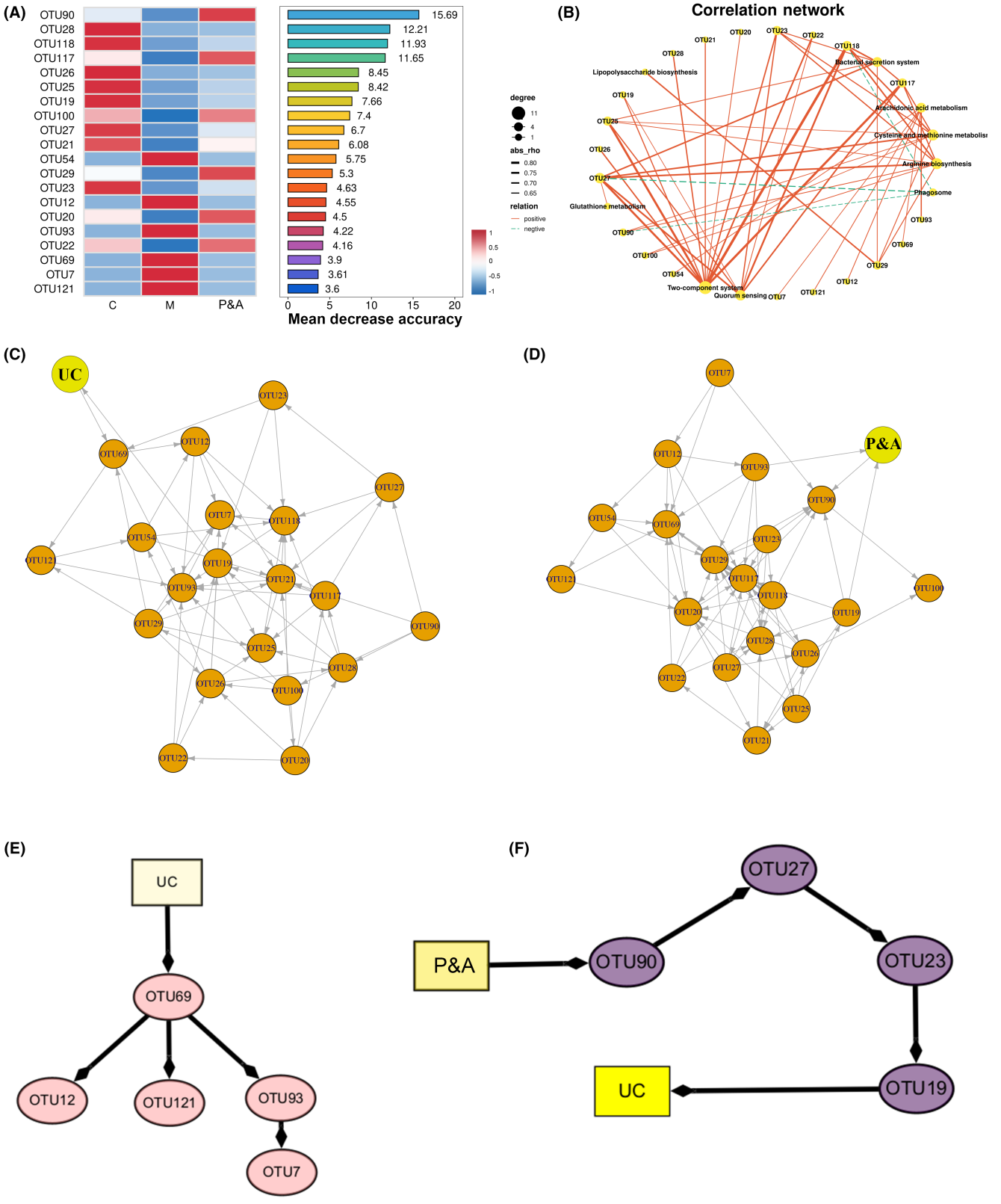

FIGURE 4 Causal relationship between key differentially expressed microbial OTUs related to inflammatory pathways. (A) Random forest model-selected top 20 OTUs contribution ranking and clustering heatmap among the three groups. (B) Correlation network diagram of top 20 OTUs and related KEGG signaling pathways. (C) Bayesian correlation network diagram of key OTUs in the model group. (D) Bayesian correlation network diagram of key OTUs in PE&AFWE group. (E) Bayesian analysis network for the causal relationship between different lumen OTUs and UC. (F) Bayesian analysis network for the causal relationship between different lumen OTUs and PE&AFWE. C, control; M, UC model; P&A, PE&AFWE group.

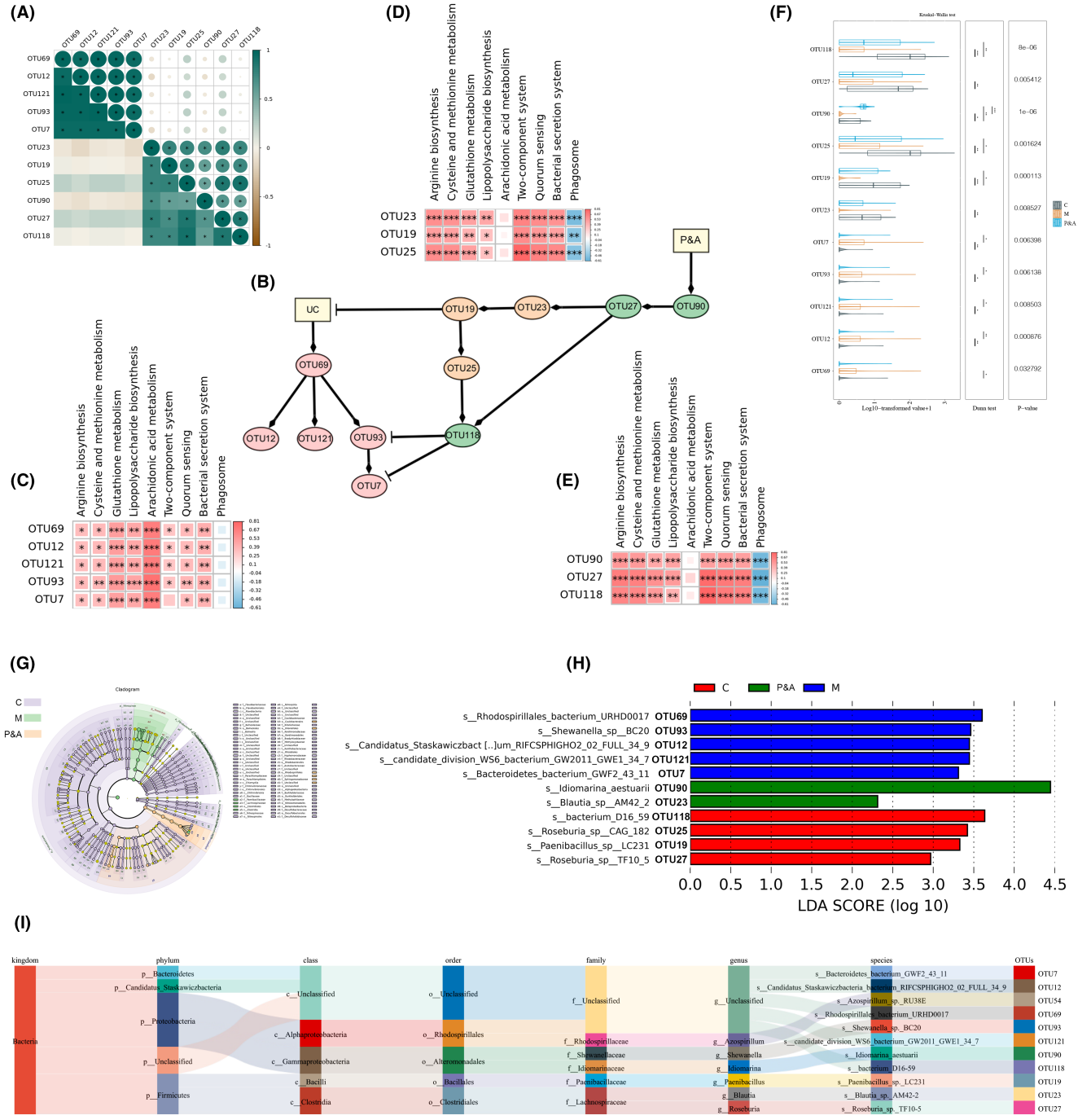

FIGURE 5 Causality of interactions between microorganisms directly regulated by UC model and drug administration groups established by Bayesian network model analysis. (A) Correlation coefficient diagram of common OTUs different between the two groups. (B) Network diagram of the interaction between the six OUTs of PE&AFWE and the five OTUs of UC. (C) Correlation diagram between directly related OTUs and arachidonic acid in UC model group. (D) Heatmap of correlation between directly related OTUs and metabolic pathways in PE&AFWE administration group. (E) Heatmap of correlation between directly related OTUs and phagosome metabolic pathway in PE&AFWE administration group. (F) STAMP analysis of key regulated OTUs in UC model and PE&AFWE administration groups. (G) LEFSe analysis showed that the two groups jointly changed the microbiota evolution map. (H) Bar chart of 11 key interaction OTU microbiota biomarkers among the three groups. (I) Analysis of the species annotation map of 11 key OTUs screened LDA > 2, $p < 0.05$. C, control; M, UC model; P&A, PE&AFWE group.

3.6 | PE&AFWE administration alleviates colitis infiltration in UC model mice

To further compare PE&AFWE with the effectiveness of classical drugs currently used in the clinical treatment of inflammatory bowel disease, we established a salazosulfapyridine (SASP) group on the basis of the three original groups, i.e. the control group ($N = 10$), the PE&AFWE group ($N = 10$), the UC model group ($N = 10$) and the SASP group ($N = 10$), as shown in Figure 6. Based on the normal intestinal mucosal structural layer, we found that (1) the disease activity index

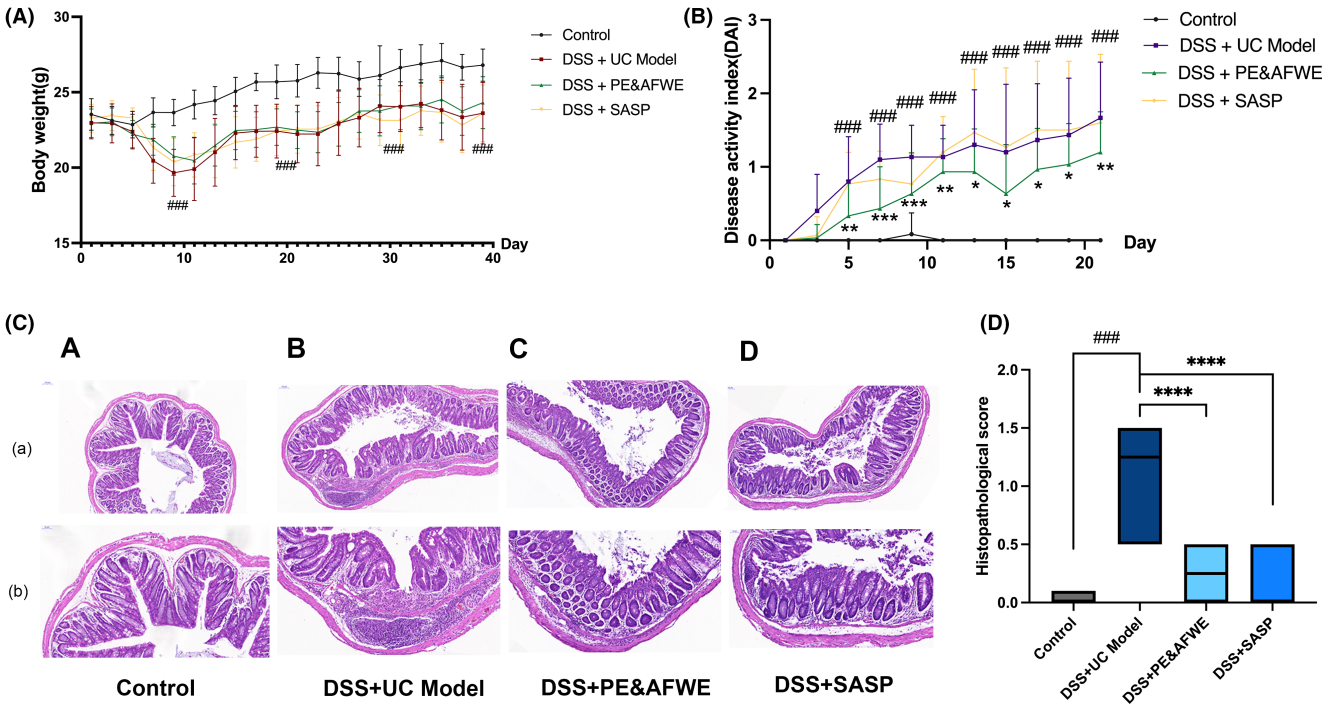

FIGURE 6 PE&AFWE administration alleviates colitis infiltration in UC model mice. (A) PE&AFWE administration alleviates the degree of inflammation in the intestine of UC model mice as shown by a weight change curve of mice. (B) Evaluation of disease activity index of a dextran sulfate sodium induced UC mouse model. (C) Pathological staining diagram of colon in control, DSS + UC model, DSS + PE&AFWE, and DSS + SASP groups. (D) Histogram of colonic pathological injury scores in control, DSS + UC model, DSS + PE&AFWE, and DSS + SASP groups; (a) the upper image is 10× (scale bar, 100 μm); (b) the lower image is 20× (scale bar, 50 μm); $N = 10$ in all groups. Compared with the control group, $^{\#}p < 0.05$, $^{\#\#}p < 0.01$, $^{\#\#\#}p < 0.001$; compared with the model group, $^{*}p < 0.05$, $^{**}p < 0.01$, $^{***}p < 0.001$, $^{****}p < 0.0001$.

(DAI) of the groups overall showed an upward trend when compared with that of the control group, among which the PE&AFWE treatment group appeared to have a low potential effect in the course of this process but the trend became similar to that of the SASP group as the treatment progressed; (2) histopathological examination at high magnification revealed the disappearance of colonic glands and inflammatory cell infiltration in the ulcerated lesions in the model group, whereas in the PE&AFWE-treated group and the SASP group, there was an intact mucosal epithelium and inflammatory infiltrated lamina propria (fewer inflammatory cells in the former/more inflammatory cells in the latter), and a decrease in the number of glands; (3), histopathological observation and scoring (HS) of the colon showed that there was a significant difference between the model group and the control group ($p < 0.001$), and that there was a significant recovery in both the SASP and the PE&AFWE groups after the administration of the drug ($p < 0.0001$).

4 | DISCUSSION

IBD is thought to result from an inappropriate and continuing inflammatory response to commensal microbes in a genetically susceptible host.[24] Histologically, ulcerative colitis shows superficial inflammatory changes limited to the mucosa and submucosa with cryptitis and crypt abscesses. Our results in the mouse model of IBD reaffirm the idea that the reduced diversity of the microbiome leads to gut microbiota dysbiosis.[25,26] Our study systematically analyzes the causal relationship between gut microbiota diversity and dysbiosis from the perspective of an animal model. Various statistics analysis methods based on PCoA, NMDS analyses, random forest, and Bayesian network models have provided compelling evidence for a causal relationship between gut microbiota diversity and inflammatory bowel disease, i.e. a causal relationship between different OTUs and UC model/PE&AFWE administration and screening for a network of OTUs that are directly related. Evidence was also obtained to indicate that OTU118 inhibits the activity of the arachidonic acid metabolic pathway, which in turn inhibits the microbial colonization of the gut by OTU93 and OTU7.

The symptoms of DSS-induced colitis in mice are similar to human UC. Acute or chronic colitis models were constructed by adjusting the concentration and frequency of DSS administration.[27,28] DSS stimulation increased the proportion of Proteobacteria in mice intestine, while PE&AFWE treatment reversed the change of Proteobacteria. These results suggest that DSS can induce UC by changing the composition and structure of intestinal gut microbiota and special microbiota, and PE&AFWE can inhibit the inflammatory response of the colon by reversing the changes to intestinal gut microbiota. The diversity of intestinal gut microbiota in UC mice stimulated by DSS decreased, with Bacteroides and Clostridium increasing significantly, and Akkermansia and Enterobacter also increasing. This

resulted in a lack of species able to produce butyrate metabolites, which in turn relates to the inflammatory response associated with intestinal diseases in mice induced by DSS.[29,30] β Diversity analysis showed that UC model mice showed obvious clustering separation through PCoA and NMDS. DSS stimulation increased the proportion of Proteobacteria and Deferribacteres in the intestinal tract of mice, and significantly reduced the abundance of Firmicutes. The relative abundance of beneficial microbial species in UC patients has been shown to be significantly reduced.[31] In this study, analysis of the differential microbiota of the UC group also showed that the overall microbial abundance of the UC group decreased compared with the normal control group of mice.

Two plant extracts were used in our study. In contrast to the use of chemical drugs in the treatment of UC, herbal medicine has the characteristics of being multi-target, low toxicity and with a low incidence of side effects. PE&AFWE, composed of *P. nudicaule* L. extract and *A. frigida* Willd. extract, is a classic prescription for the treatment of UC. Its clinical application has proved that it can effectively treat UC, and the recurrence rate of UC treated with PE&AFWE is low.[32] However, the mechanism by which PE&AFWE attenuates UC remains to be proved. We found that compared with the untreated UC model group, PE&AFWE significantly alleviated the disease activity index (DAI), improved the symptoms of hematochezia and diarrhea, and reversed the inflammatory cell infiltration. Firmicutes and Bacteroidetes were shown to be the two largest microbial communities in this study and the proportion of Firmicutes/Bacteroidetes found in this study is consistent with that previously reported[33]. The proportion of Firmicutes/Bacteroidetes decreased in UC due to colon injury. Idiomarina has unique physiological fatty acids.[34] Bayesian network analysis shows that it is also an important gut microbe that directly regulates the abundance of other gut microbiota after administration. It is speculated that increasing the abundance of *idiomarina* after administration is helpful to the increase of short chain fatty acids.

Among the directly related species screened by the random forest and Bayesian causality network after PE&AFWE administration, three species belong to the family Lachnospiraceae. It is reported that members of the family Lachnospiraceae have a wide range of metabolic functions, including the synthesis of short chain fatty acids (including raw propionate, butyrate and other metabolites), the degradation of mucin, and the metabolism of sugar and aromatic amino acids.[35–37] They are negatively correlated with the concentration of pro-inflammatory cytokines, and are related to the inflammatory remission of IBD. Members of the family Lachnospiraceae play an active role in intestinal homeostasis.[38,39]

In this study, PE&AFWE administration significantly reversed the reduced abundance of Clostridiales in mice in the UC model group. According to the correlation coefficient analysis, the differentially regulated gut microbiota after PE&AFWE administration can be divided into two categories, one is mainly enriched in arachidonic acid (ko00590) and the other is mainly related to phagosomes (ko04145). Arachidonic acid mediates adipoinflammation, and studies have shown that regulating gut microbiota metabolism through diet can alleviate inflammation, which is consistent with the results of this study.[40] OTU69, OTU12, OTU121, OTU93 and OTU7 directly regulated by UC were highly correlated with the arachidonic acid pathway, and there was no significant correlation between OTUs directly regulated by PE&AFWE administration and arachidonic acid (OTU69 [*Rhodospirillales bacterium URHD0017*], OTU12 [*Candidatus Staskawiczbacteria bacterium RIFCSPHIGHO2_02_FULL_34_9*], OTU121 [*Candidate_division_WS6_bacterium_GW2011_GWE1_34_7*], OTU93 [*Shewanella* sp. BC20] and OTU7 [*Bacteroidetes bacterium* GWF2_43_11]).

The ability of phagosomes to prevent bacterial infection depends on their continuous interaction with the microbial community, which is the key to determining whether phagosomes will be infected by pathogens. The macrophage population in the intestinal lamina propria is the most abundant in the immune population, mainly nonmigratory macrophages, belonging to the functional M2 subtype, which can produce a large number of IL-10 cytokines. Studies have shown that most of the Tregs in the colon are accumulated by the microbiota in the colon and antigen-specific interactions. In this study, the microbial gene functions of mice treated with PE&AFWE mainly involved arachidonic acid (ko00590) and phagosome (ko04145), revealing their close correlation with reducing antiviral infection and inhibiting the release of pro-inflammatory factors. The Bayesian causal network analysis graph in this study intuitively shows the interaction relationship of each biomarker analyzed by LEfSe, respectively, in the UC model and PE&AFWE groups. The directly linked biomarkers represent the intestinal species that have a direct effect on the intestinal microbial dysbiosis in UC model mice, that is, the intestinal species most closely related to the UC model or PE&AFWE after administration. This study found that PE&AFWE can regulate the dysbiosis of gut microbiota and directly affect *Idiomarina aestuarii* from the Idiomarinaceae family and *Blautia* sp. AM42-2 from the Lachnospiraceae family.

This study confirms by random forest and Bayesian network analyses the causal effect of gut microbiota on dysbiosis in IBD, and also provides evidence of histopathological changes. The study also identified five opportunistic pathogens in three phyla that directly contribute to IBD, and the arachidonic acid metabolic pathway, an inflammatory pathway influenced by *Idiomarina aestuarii*, Significant histopathological improvement was seen when inflammatory bowel disease was treated with PE&AFWE, with decreased abundance of Proteobacteria gut microbiota. The findings of this study expand our understanding of the microbiota–IBD relationship and suggest that PE&AFWE could be a candidate for further research in the development of gut therapeutics for IBD.

AUTHOR CONTRIBUTIONS

Qianhui Fu carried out experiments and analyzed data and wrote the manuscript; Xiaoqin Ma, Mengni Shi, Shuchun Li contributed to some experiments; Qianhui Fu, Xiaoqin Ma, Mengni Shi Tianyuan Song were responsible for sample collection and processing; Shuchun Li and Jian Cui supervised and designed the research. All the authors approved the final version of the manuscript.

ACKNOWLEDGMENTS

This work was supported by the National Natural Science Foundation of China (Grant No. 81774449).

CONFLICT OF INTEREST STATEMENT

The authors declare that there are no conflicts of interest to disclose.

ETHICS STATEMENT

All animal experiments were approved, and the experimental protocol was carried out according to the guidelines formulated by the ethics committee of China University for Nationalities (protocol number: ECMUC2021006AO).

ORCID

Qianhui Fu https://orcid.org/0000-0002-0797-0988

REFERENCES

1. Ley RE, Ley RE, Peterson DA, et al. Ecological and evolutionary forces shaping microbial diversity in the human intestine. *Cell*. 2006;124:837-848. doi:10.1016/j.cell.2006.02.017
2. Li X, Wang X, Wang Z, Guan J. Systems biology of the gut: the interplay of food, microbiota and host at the mucosal interface. *Anim Model Exp Med*. 2023;6(6):598-608. doi:10.1002/ame2.12351
3. Shade A, Shade A, Handelsman J, Handelsman J. Beyond the Venn diagram: the hunt for a core microbiome. *Environ Microbiol*. 2012;14:4-12. doi:10.1111/j.1462-2920.2011.02585.x
4. Ichinohe T, Pang IK, Kumamoto Y, et al. Microbiota regulates immune defense against respiratory tract influenza a virus infection. *Proc Natl Acad Sci USA*. 2011;108(13):5354. doi:10.1073/pnas.1019378108
5. Abt MC, Osborne LC, Monticelli LA, et al. Commensal bacteria calibrate the activation threshold of innate antiviral immunity. *Immunity*. 2012;37(1):158-170. doi:10.1016/j.immuni.2012.04.011
6. Wardwell LH, Wardwell L, Huttenhower C, Huttenhower C, Garrett WS, Garrett WS. Current concepts of the intestinal microbiota and the pathogenesis of infection. *Curr Infect Dis Rep*. 2011;13:28-34. doi:10.1007/s11908-010-0147-7
7. Watanabe K, Itoh K, Park SH, et al. Resistin-like molecule beta, a colonic epithelial protein, exhibits antimicrobial activity against *Staphylococcus aureus* including methicillin-resistant strains. *Surg Today*. 2020;50(8):920-930. doi:10.1007/s00595-020-01974-z
8. Zafar H, Saier MH. Gut *Bacteroides* species in health and disease. *Gut Microbes*. 2021;13(1):1848158. doi:10.1080/19490976.2020.1848158
9. Maynard CL, Maynard CL, Elson CO, et al. Reciprocal interactions of the intestinal microbiota and immune system. *Nature*. 2012;489:231-241. doi:10.1038/nature11551
10. Borowitz SM. The epidemiology of inflammatory bowel disease: clues to pathogenesis? *Front Pediatr*. 2023;10:1103713. doi:10.3389/fped.2022.1103713
11. Tarar ZI, Zafar MU, Farooq U, et al. Burden of depression and anxiety among patients with inflammatory bowel disease: results of a nationwide analysis. *Int J Color Dis*. 2022;37(2):313-321. doi:10.1007/s00384-021-04056-9
12. Loddo I, Romano C. Inflammatory bowel disease: genetics, epigenetics, and pathogenesis. *Front Immunol*. 2015;6:551. doi:10.3389/fimmu.2015.00551
13. Garber A, Garber A, Regueiro M, Regueiro M. Extraintestinal manifestations of inflammatory bowel disease: epidemiology, etiopathogenesis, and management. *Curr Gastroenterol Rep*. 2019;21:31. doi:10.1007/s11894-019-0698-1
14. Hedin C, Hedin C, Hedin C, et al. The pathogenesis of extraintestinal manifestations: implications for IBD research, diagnosis, and therapy. *J Crohns Colitis*. 2019;13:541-554. doi:10.1093/ecco-jcc/jjy191
15. Sokol H, Sokol H, Lay C, et al. Analysis of bacterial bowel communities of IBD patients: what has it revealed? *Inflamm Bowel Dis*. 2008;14:858-867. doi:10.1002/ibd.20392
16. DeGruttola AK, Low D, Mizoguchi A, Mizoguchi E. Current understanding of dysbiosis in disease in human and animal models. *Inflamm Bowel Dis*. 2016;22(5):1137-1150. doi:10.1097/MIB.0000000000000750
17. Paik J, Meeker S, Hsu CC, et al. Validation studies for germ-free Smad3−/− mice as a bio-assay to test the causative role of fecal microbiomes in IBD. *Gut Microbes*. 2020;11(1):21-31. doi:10.1080/19490976.2019.1611151
18. Casén C, Vebø HC, Sekelja M, et al. Deviations in human gut microbiota: a novel diagnostic test for determining dysbiosis in patients with IBS or IBD. *Aliment Pharmacol Ther*. 2015;42(1):71-83. doi:10.1111/apt.13236
19. Briggs K, Tam A, Housseau F, Melia J, Pardoll D. The effects of biologic and small molecule inhibitor therapy on the mucosal immune system in ulcerative colitis. *Inflamm Bowel Dis*. 2023;29(Supplement_1):S45-S46. doi:10.1093/ibd/izac247.083
20. Ursomanno BL, Cohen RE, Levine MJ, Yerke LM. P064 treatment of crohn's disease and ulcerative colitis with proton pump inhibitors: effect on bone loss at dental implants. *Inflamm Bowel Dis*. 2019;25(Supplement_1):S30-S31. doi:10.1093/ibd/izy393.070
21. Ishida N, Onoue S, Miyazu T, et al. Further research on the clinical relevance of the ulcerative colitis colonoscopic index of severity for predicting 5-year relapse. *Int J Color Dis*. 2021;36(12):2661-2670. doi:10.1007/s00384-021-04009-2
22. Murray A, Nguyen TM, Parker CE, Feagan BG, MacDonald JK. Oral 5-aminosalicylic acid for maintenance of remission in ulcerative colitis. *Cochrane Database Syst Rev*. 2020;8(8):CD000544. doi:10.1002/14651858.CD000544.pub5
23. Nishida A, Nishida A, Nishida A, et al. Can control of gut microbiota be a future therapeutic option for inflammatory bowel disease. *World J Gastroenterol*. 2021;27:3317-3326. doi:10.3748/wjg.v27.i23.3317
24. Liu TC, Liu TC, Stappenbeck TS, Stappenbeck TS. Genetics and pathogenesis of inflammatory bowel disease. *Annu Rev Pathol*. 2016;11:127-148. doi:10.1146/annurev-pathol-012615-044152
25. Frank DN, Frank DN, Amand ALS, et al. Molecular-phylogenetic characterization of microbial community imbalances in human inflammatory bowel diseases. *Proc Natl Acad Sci USA*. 2007;104:13780-13785. doi:10.1073/pnas.0706625104
26. Sartor RB, Sartor RB, Wu GD, Wu GD. Roles for intestinal bacteria, viruses, and fungi in pathogenesis of inflammatory bowel diseases and therapeutic approaches. *Gastroenterology*. 2017;152:327-339.e4. doi:10.1053/j.gastro.2016.10.012
27. Wu Y, Ran L, Yang Y, et al. Deferasirox alleviates DSS-induced ulcerative colitis in mice by inhibiting ferroptosis and improving intestinal microbiota. *Life Sci*. 2023;314:121312. doi:10.1016/j.lfs.2022.121312
28. Wirtz S, Popp V, Kindermann M, et al. Chemically induced mouse models of acute and chronic intestinal inflammation. *Nat Protoc*. 2017;12(7):1295-1309. doi:10.1038/nprot.2017.044
29. Eichele DD, Kharbanda KK. Dextran sodium sulfate colitis murine model: an indispensable tool for advancing our understanding of inflammatory bowel diseases pathogenesis. *World J Gastroenterol*. 2017;23(33):6016-6029. doi:10.3748/wjg.v23.i33.6016
30. Xu HM, Huang HL, Liu YD, et al. Selection strategy of dextran sulfate sodium-induced acute or chronic colitis mouse models based on gut microbial profile. *BMC Microbiol*. 2021;21(1):279. doi:10.1186/s12866-021-02342-8
31. Varela E, Manichanh C, Gallart M, et al. Colonisation by *Faecalibacterium prausnitzii* and maintenance of clinical

remission in patients with ulcerative colitis. *Aliment Pharmacol Ther*. 2013;38(2):151-161. doi:10.1111/apt.12365
32. Jian C, Zong-Ran P, Li-Ge-Ma DE, Bi-Nan LU, Wei-Zhi L. Clinical observation on Garidisan in 60 patients with ulcerative colitis. *Tianjin J Tradit Chin Med*. 2012;29(11):17-18.
33. Li X, Wang X, Wang Z, Guan J. Baizhu-Baishao herb pair ameliorates functional constipation and intestinal microflora disorder in rats. *Anim Model Exp Med*. 2023;6(6):598-608. doi:10.1002/ame2.12351
34. Choi DH, Cho BC. Idiomarina seosinensis sp. nov., isolated from hypersaline water of a solar saltern in Korea. *Int J Syst Evol Microbiol*. 2005;55(1):379-383.
35. Reichardt N, Duncan SH, Young P, et al. Phylogenetic distribution of three pathways for propionate production within the human gut microbiota. *ISME J*. 2014;8(6):1323-1335. doi:10.1038/ismej.2014.14
36. Sasaki K, Inoue J, Sasaki D, et al. Construction of a model culture system of human colonic microbiota to detect decreased *Lachnospiraceae* abundance and Butyrogenesis in the feces of ulcerative colitis patients. *Biotechnol J*. 2019;14(5):e1800555. doi:10.1002/biot.201800555
37. Wu M, Chi C, Yang Y, et al. Dynamics of gut microbiota during pregnancy in women with TPOAb-positive subclinical hypothyroidism: a prospective cohort study. *BMC Pregnancy Childbirth*. 2022;22(1):1-14.
38. Smith PM, Howitt MR, Panikov N, et al. The microbial metabolites, short-chain fatty acids, regulate colonic Treg cell homeostasis. *Science*. 2013;341(6145):569-573. doi:10.1126/science.1241165
39. Arpaia N, Campbell C, Fan X, et al. Metabolites produced by commensal bacteria promote peripheral regulatory T-cell generation. *Nature*. 2013;504(7480):451-455. doi:10.1038/nature12726
40. Miyamoto J, Igarashi M, Watanabe K, Karaki SI, Kimura I. Gut microbiota confers host resistance to obesity by metabolizing dietary polyunsaturated fatty acids. *Nat Commun*. 2019;10(1):836-840.

SUPPORTING INFORMATION

Additional supporting information can be found online in the Supporting Information section at the end of this article.

How to cite this article: Fu Q, Ma X, Li S, Shi M, Song T, Cui J. New insights into the interactions between the gut microbiota and the inflammatory response to ulcerative colitis in a mouse model of dextran sodium sulfate and possible mechanisms of action for treatment with PE&AFWE. *Anim Models Exp Med*. 2024;7:83-97. doi:10.1002/ame2.12405